Kinetic Adsorption of Hazardous Methylene Blue from Aqueous Solution onto Iron-Impregnated Powdered Activated Carbon[#]

Athit Phetrak[1*], Sirirat Sangkarak[1], Sumate Ampawong[2], Suda Ittisupornrat[3], and Doungkamon Phihusut[4]

[1]Department of Social and Environmental Medicine, Faculty of Tropical Medicine, Mahidol University, Bangkok 10400, Thailand
[2]Department of Tropical Pathology, Faculty of Tropical Medicine, Mahidol University, Bangkok 10400, Thailand
[3]Environmental Research and Training Center, Department of Environmental Quality Promotion, Bangkok 10400, Thailand
[4]Environmental Research Institute, Chulalongkorn University, Bangkok 10330, Thailand

ARTICLE INFO

Received: 7 Feb 2019
Received in revised:
30 May 2019
Accepted: 12 Jun 2019
Published online:
4 Jul 2019
DOI: 10.32526/ennrj.17.4.2019.33

Keywords:
Adsorption/ Dye removal/ Iron-Impregnated Powdered Activated Carbon/ Methylene blue

*** Corresponding author:**
E-mail:
athit.phe@mahidol.ac.th;
athit.phetrak@gmail.com

ABSTRACT

In this study, iron-impregnated powdered activated carbon (Fe-PAC) prepared using chemical co-precipitation techniques was used as an adsorbent for methylene blue (MB) removal in a batch experiment. The analysis of transmission electron microscopy, scanning electron microscopy with energy dispersive spectroscopy showed that iron oxide particle was substantially distributed into the surface of the adsorbent, suggesting that Fe-PAC was successfully synthesized. The results showed that fast and efficient adsorption of MB by Fe-PAC was achieved, with a relative short contact time of 10 min and MB adsorption capacity of 51 mg/g. The kinetic adsorption of MB on Fe-APC adsorbent was well described by a pseudo-second-order model. Concurrently, the analysis of intraparticle diffusion model suggests that intraparticle diffusion is not the only rate-limiting step of MB molecules adsorption by Fe-PAC adsorbent. The elevated temperature conditions also improved the removal efficiency of MB. Thermodynamic parameters exhibited by the MB adsorption process onto Fe-PAC were endothermic and spontaneous. The findings of the present work indicate that Fe-PAC can be a potentially effective adsorbent for MB removal in wastewater due to its fast and efficient MB adsorption, and separation in wastewater treatment systems.

1. INTRODUCTION

Currently, there are rising concerns of environmental and public health problems caused by hazardous pollutant of dyes due to their toxic, mutagenic, allergenic and carcinogenic properties. Many industries, such as textile, printing, and plastic, incorporate dyes and pigments in to their production processes. Consequently, colored wastewaters have been found in treatment processes because of dyes used in industrial product and washing processes. Dyeing industries discharge between 30,000 and 150,000 tons of dyes per year into receiving waters (Anjaneya et al., 2013). Thus, colored wastewater released into natural waters is not only aesthetically displeasing but also detrimental to natural water quality.

In the past, various technologies have been proposed for eliminating dyes from wastewater, namely, adsorption (Li et al., 2018; Wong et al., 2016; Wu et al., 2014), membrane filtration (Rashidi et al., 2015), ion exchange (Karcher et al., 2002) and biological treatment (Anjaneya et al., 2013). Among these, adsorption by activated carbon, such as powdered activated carbon (PAC), is one of the most effective techniques for water decontamination due to its operational simplicity, and high removal efficiency of pollutants. Nevertheless, the limitation of the use of PAC as an adsorbent in water and wastewater treatment could be the result of its separation due to low settling rates. Concurrently, membrane filtration clogging and the regeneration of used adsorbent are also challenges of PAC application. Therefore, there is a need for the development of a novel adsorbent for pollutant removal to overcome these limitations.

Recently, the use of iron oxide particles has attracted considerable research attention in the field of water and wastewater treatment because of its

[#]This paper was selected from the 3rd Environment and Natural Resources International Conference (ENRIC 2018) which was held during 22-23 November, 2018 in Thailand

high adsorption capacity and fast separation using an external magnetic separator (Rajput et al., 2016; Kitkaew et al., 2018). The combination of PAC and iron oxide particles as iron-impregnated powdered activated carbon (Fe-PAC) could be thus an ideal adsorbent for pollutant removal from water due to self-settling and high adsorption capacity. In this study, we developed Fe-PAC as an adsorbent in laboratory scale employing a simple chemical co-precipitation method and then using it to remove methylene blue (MB) as a model dye compound in aqueous solution. Batch adsorption of MB onto Fe-PAC was carried out as a function of adsorption time and equilibrium temperature conditions. MB removal mechanism by Fe-PAC and its adsorption capacity were also examined. The results from this study can provide useful information for the removal of MB from wastewater of dye industries.

2. METHODOLOGY

2.1 Preparation of Fe-PAC adsorbent

The PAC (received from Sigma-Aldrich, Singapore) was washed with Milli-Q water to remove impurities as received-PAC. The Fe-PAC adsorbent was prepared by a chemical co-precipitation method, adapted from our previous method of Kitkaew et al. (2018). Briefly, 18.3 g of $FeSO_4 \cdot 7H_2O$, 33.3 g of $FeCl_3 \cdot 6H_2O$, 25 g of PAC and 1,000 mL of Milli-Q water were combined in a 2,000-mL beaker and mixed by magnetic stirrer. The mixed solution was heated to 65±2 °C and then cooled down to below 40 °C before adding of 5 N NaOH to increase the pH solution to 10-11. The resulting suspension was stirred constantly for 1 h and then rested overnight to precipitate. Subsequently, the supernatant was discarded and the adsorbent suspension was rinsed thrice with 1,000 mL of Milli-Q water and twice with ethanol. The adsorbent suspension was then transferred into 50-mL conical centrifuge tubes and centrifuged at 3,000 rpm for 5 min. The pellet was harvested, dried at 70-75 °C in an oven for 48 h and then manually ground and sieved to obtain a 20-50 mesh fraction which was kept in an air-tight container until further use. The surface morphology and elemental compositions of the adsorbent were characterized using transmission electron microscopy (TEM) (Hitachi-HT7700) and scanning electron microscopy (SEM) coupled with an energy dispersive spectrometer (SEM-EDS) (Hitachi-SU3500, Japan).

2.2 MB adsorption experiments

Analytical grade of MB (chemical formula of $C_{16}H_{18}N_3ClS \cdot 2H_2O$) was obtained from Ajax Finechem. The stock of MB solution of 1,000 mg/L was made by dissolving an exact amount of MB in Milli-Q water at room temperature (25±1 °C). The experimental MB concentrations were thereafter diluted to require concentration using Milli-Q water.

Time-dependent adsorption experiments were conducted using the bottle-point-technique. The pre-weighted amount of 100-mg Mag-PAC was added into a 100-mL flask containing MB solution of 50 mL to obtain a Fe-PAC dose of 2.0 g/L, with initial MB concentration of 100 mg/L and initial pH of 8.13. Consequently, the mixed solution was agitated at 150 rpm in a horizontal shaking incubator at 25 °C for 120 min.

Separately, from time-dependent adsorption experiments, adsorption of MB on Fe-PAC was performed at various equilibrium temperature conditions (15-65 °C) to investigate the effect of temperature on MB adsorption. Fe-PAC adsorbent of 100 mg was introduced to a series of 100-mL Erlenmeyer flasks. A MB solution with concentration of 200 mg/L was incubated at the target temperature conditions for a few hours before being added to each flask. Thereafter, the flasks were completely sealed with plastic sheets to avoid water evaporation during adsorption at specific temperature conditions. Subsequently, the prepared flasks were transferred in an incubator shaker at a pre-set temperature. This experimental condition was carried out at an adsorbent dose of 2 g/L, initial pH of 6.1, initial MB concentration of 200 mg/L, agitation speed of 150 rpm and adsorption time of 20 h. The use of MB concentration of 100-200 mg/L and Fe-PAC dose of 2 g/L in our study are within the ranges of dye adsorption documented in previous studies (Phihusut and Chantharat, 2017; Novais et al., 2018). At specific adsorption times, each bottle was opened and an aliquot sample was filtered through a pre-rinsed 0.45 µm membrane nylon filter. The MB concentration in aqueous solution before and after adsorption by Fe-PAC was determined by UV-Visible spectrophotometer (U-2700, Shimadzu) at 668 nm. Each adsorption experiment was carried out in duplicate samples under identical conditions. The average value was reported with standard deviation. The removal rates of MB (%) and its adsorption capacity at t time; q_t (mg/g) were

examined following the equations of 1 and 2, respectively.

$$\text{MB removal (\%)} = \frac{C_o - C_e}{C_o} \times 100 \quad (1)$$

$$\text{Adsorption capacity at time } (q_t) = \frac{C_o - C_t}{m} \times V \quad (2)$$

Where C_o and C_e are the initial and equilibrium MB concentration in the solution (mg/L), respectively, V is the solution volume (L) and m is the mass of Fe-PAC adsorbent (g).

In addition, the results of MB adsorption by Fe-PAC were fitted with pseudo-first-order, pseudo-second-order and intraparticle diffusion models, which are expressed in equations of 3 (Lagergren, 1898), 4 (Ho et al., 2000), and 5 (Weber and Morris, 1963), respectively.

$$\ln(q_e - q_t) = \ln q_e - k_1 t \quad (3)$$

$$\frac{t}{q_t} = \frac{1}{k_2 q_e^2} + \frac{t}{q_e} \quad (4)$$

$$q_t = k_{diff} \times t^{0.5} + C \quad (5)$$

Where q_e and q_t are the adsorption amounts of MB (mg/g) at equilibrium and time t (min), respectively, and k_1 (1/min), k_2 (g/mg.min) and k_{diff} (mg/g.$t^{0.5}$) are the rate constants of the pseudo-first-order, pseudo-second-order adsorption, and intraparticle diffusion respectively. C is a constant (mg/g).

The effect of temperature (288, 298, 308, 318, 328, and 338 K) on thermodynamic parameters for MB adsorption onto Fe-PAC was also investigated in this work. The calculation of Gibbs free energy (ΔG^0), enthalpy (ΔH^0) and entropy (ΔS^0) were determined from the following equations;

$$K_c = \frac{(C_o - C_t)}{C} \times \frac{V}{W} \quad (6)$$

$$\Delta G^o = -RT \ln K_c \quad (7)$$

$$\ln K_c = \frac{\Delta S^o}{R} - \frac{\Delta H^o}{RT} \quad (8)$$

Where K_C is equilibrium constant of MB adsorption onto Fe-PAC. R is the universal gas constant (8.314 J/ mol·K), while T is the absolute temperature (K) of adsorption system.

3. RESULTS AND DISCUSSION

3.1 Characterization of Fe-PAC adsorbent

The structural analysis of Fe-PAC was studied at high magnification using TEM as shown in Figure 1. The images of Fe-PAC adsorbent, synthesized by chemical co-precipitation method, clearly showed that iron oxide particles are embedded into the activated carbon powder pores. This corresponded with morphological observation using SEM (Figure 2) with iron oxide particles well dispersed covering the PAC matrix. However, the result was also consistent with EDS results as seen in Table 1, showing elemental composition of the adsorbent at 36.2% of carbon, followed by 33.3% of oxygen, 29.4% iron, and 1.1% sodium. This phenomenon can be hypostasized that reduction of specific surface area of the adsorbent after iron impregnation may result in pore blockage of iron oxide particles onto PAC pores (Han et al., 2015; Mohan et al., 2011; Shang et al., 2016). In addition, this magnetizing process can also lead to decreased pH value at the point of zero charge (pH_{pzc}) of Fe-PAC. Normally, pH_{pzc} of PAC adsorbent was higher than 8.7 (Han et al., 2015; Punyapalakul and Takizawa, 2006; Suriyanon et al., 2015), whereas pH_{pzc} of iron oxide adsorbent was ranged from 5.0 to 7.4 (Lohwacharin et al., 2014; Rajput et al., 2016). Thus, it can be implied that pH_{pzc} of Fe-PAC could be reduced as compared with PAC adsorbent. This is because the surface of PAC was oxidized by adding iron precursors during the process of impregnation (Borah et al., 2009).

Table 1. Elemental composition of the Fe-PAC adsorbent

Element	Line	Weight (%)	Atomic (%)
Carbon	K Serie	36.2	53.2
Oxygen	K Serie	33.3	36.7
Iron	L Serie	29.4	9.3
Sodium	K Serie	1.1	0.8

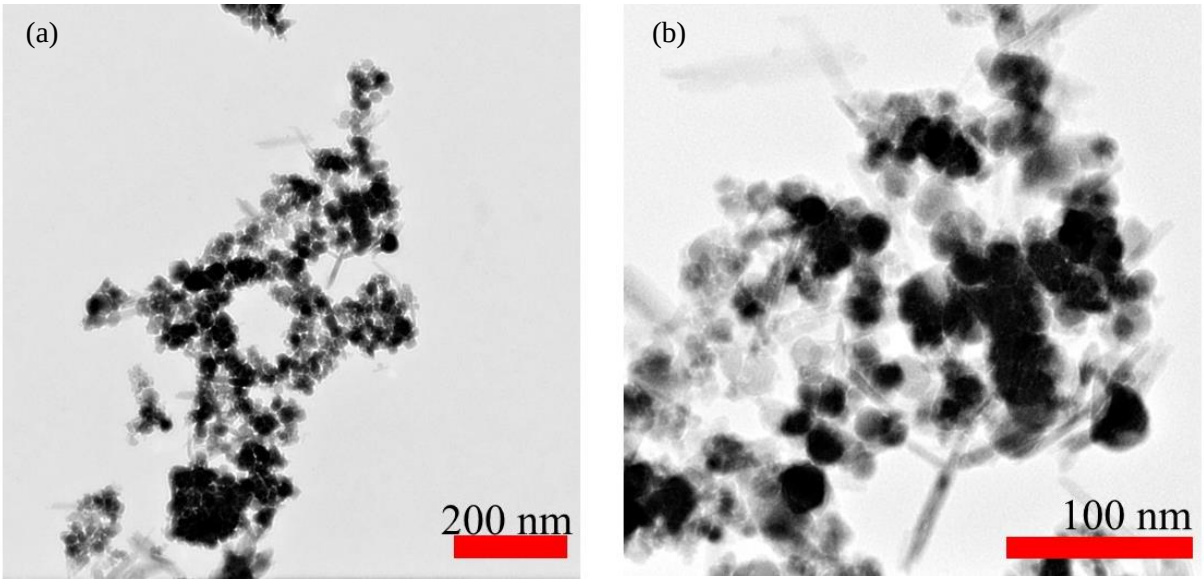

Figure 1. TEM images of Fe-PAC at (a) ×20,000 and (b) ×70,000 magnification

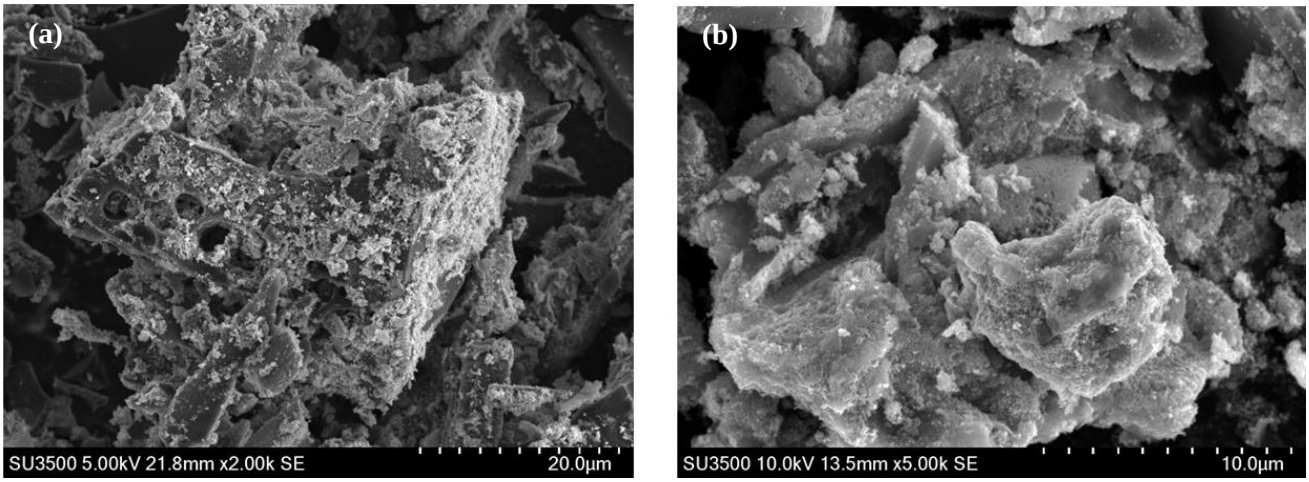

Figure 2. SEM images of Fe-PAC at (a) ×2,000 and (b) ×5,000 magnification.

3.2 Effect of adsorption time

Equilibrium adsorption time is an important factor in designing a wastewater treatment unit. The plot of MB removal and its adsorption capacity as a function of adsorption time is shown in Figure 3. It is noteworthy that the removal rate of MB and its adsorption capacity have been affected by adsorbent dose. In this study, the adsorbent dose of 2 g/L was selected to remove MB in aqueous solution. This applied dosage was similar to adsorption dosage used in other studies (Naeem et al., 2017; Novais et al., 2018). It can be observed that MB removal and its adsorption capacity was improved with elevated adsorption time. A fast uptake of the adsorbed amount of MB had been found at an 89% removal rate within a few minutes of adsorption time. This is because adsorption sites are more available during the initial state of adsorption (Fu et al., 2015). Subsequently, the MB removal rate was further increased to 99% at 10 min and then reached a plateau, indicating a reduction of accessible vacant adsorption sites. The trend of MB adsorption capacity was similar to the removal rate of MB, reaching an equilibrium adsorption state at 10 min of contact time, with MB adsorption capacity of 51 mg/g. This suggests that equilibrium achieved with Fe-PAC for MB adsorption is within 10 min, which is substantially faster than those reported in published research studies (Naeem et al., 2017; Phihusut and Chantharat, 2017; Wong et al., 2016).

This may be the main novelty of this work. Moreover, Fe-PAC adsorbent has benefits of more various functional groups compared to PAC adsorbent, resulting in enhanced pollutant removal possibly due to the dispersed iron oxide coated on PAC (Park et al., 2015). In addition, simple and quick separation from treatment processes may be achieved from Fe-PAC adsorbent by introducing an external magnetic field. Obtained results of rapid adsorption time under these experimental conditions indicate that Fe-PAC has high removal efficiency with MB molecules in aqueous solution.

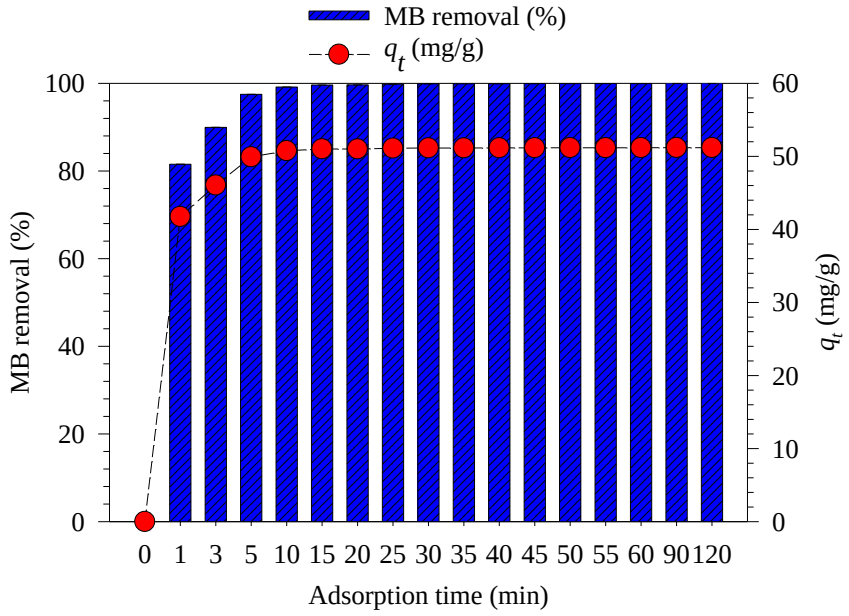

Figure 3. Influence of adsorption time on the removal efficiency of MB by Fe-PAC.

3.3 Kinetic adsorption of MB

To further investigate the kinetic rate constant of MB adsorption onto Fe-PAC and its removal mechanism, the adsorption data was applied to kinetic adsorption models; namely, pseudo-first order model, pseudo-second order model and intraparticle diffusion mode. The results of kinetic parameters of MB adsorption onto Fe-PAC adsorbent are presented in Table 2. It can be observed from Figure 4(a)-(b) that the correlation coefficient (R^2) of pseudo-second order model (R^2 closed to 1.000) is higher than that of pseudo-first order model (R^2=0.908). Additionally, the theoretical value of adsorption capacity for pseudo-second order model (q_e= 51.282 mg/g) was similar to that of the experimental equilibrium adsorption capacity (q_e=51.183 mg/g) (Table 2). Data indicates that the adsorption of MB onto Fe-PAC was fitted well with the pseudo-second-order-model, confirming that chemisorption, involving electro-static interaction between MB molecules and Fe-PAC, is a rate-limiting step (Abuzerr et al., 2018; Phihusut and Chantharat, 2017).

In this study, the intraparticle diffusion model was also employed to further describe contributions of the sorption mechanism of MB molecules onto Fe-PAC with results summarized in Figure 4(c) and Table 2. As found in Figure 4(c), the plot between q_t and adsorption time ($t^{0.5}$) displayed two straight lines, which did not pass through the origin, suggesting that intraparticle diffusion was not the only rate-controlling step. Multiple steps of diffusion mechanisms are included in MB adsorption onto Fe-PAC which is consistent with findings by others (Li et al., 2018; Pathania et al., 2017). Considering the Figure 4(c), the slope of the first straight line ($k_{diff\text{-}1}$=6.555 mg/g·min$^{0.5}$) was considerably higher than that of the slope of the second straight line ($k_{diff\text{-}1}$=0.041 mg/g·min$^{0.5}$). This suggests that sorption rate of external mass transfer was relatively faster than the rate of intraparticle diffusion.

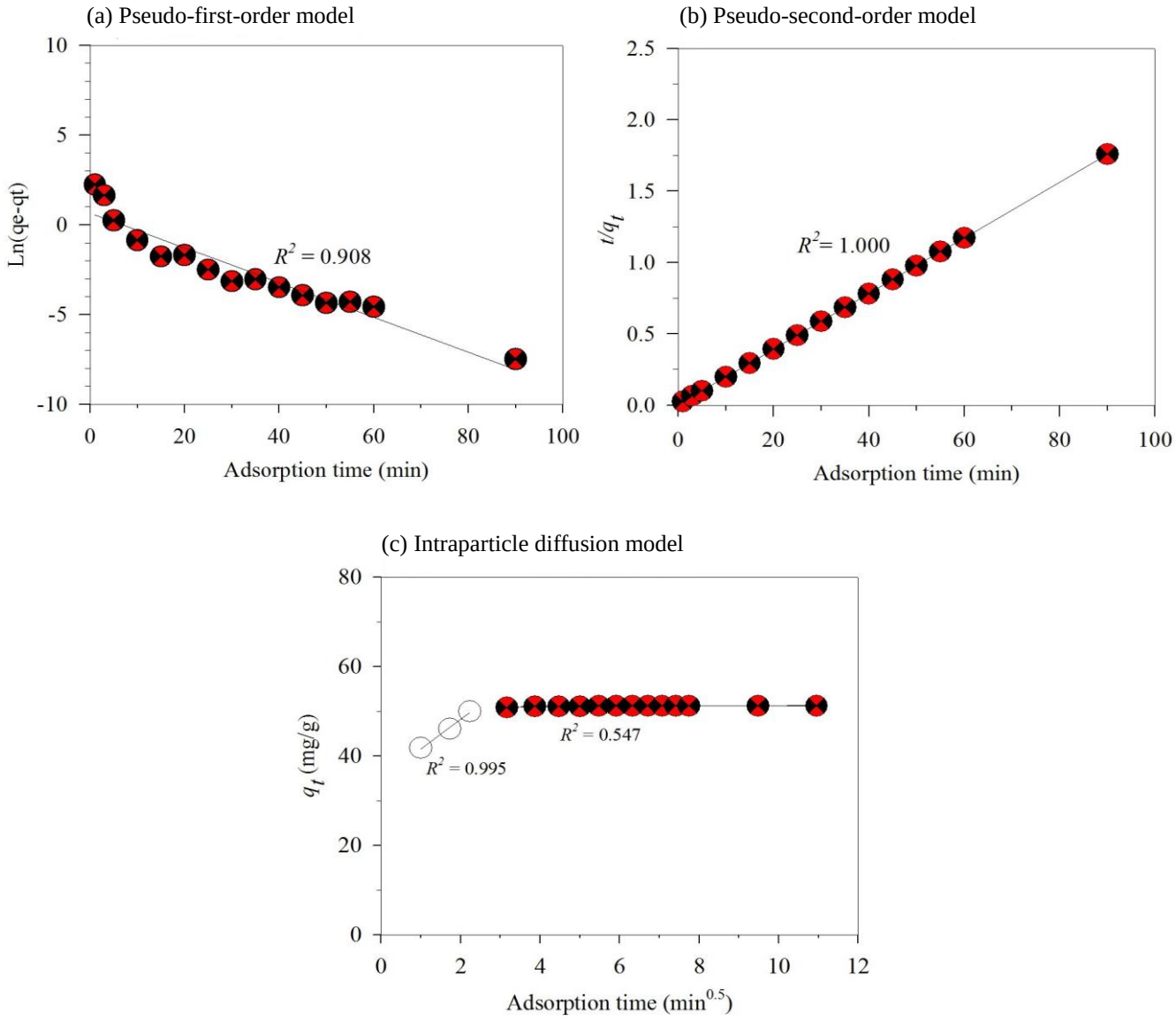

Figure 4. Kinetic adsorption models of MB by Fe-PAC (a) pseudo-first-order-model, (b) pseudo-second-order-model, and (c) intraparticle diffusion model.

Table 2. The parameters of kinetic adsorption of MB on Fe-PAC.

Kinetic adsorption models	Parameters	Values
Experimental results	q_{exp} (mg/g)	51.183
Pseudo-first-order model	q_{cal} (mg/g)	1.938
	k_1 (L/min)	0.097
	R^2	0.908
Pseudo-second-order model	q_{cal} (mg/g)	51.282
	k_2 (g/mg·min)	0.127
	R^2	1.000
Intraparticle diffusion model	K_{diff-1} (mg/g·min$^{0.5}$)	6.555
	R^2	0.995
	K_{diff-2} (g/mg·min$^{0.5}$)	0.041
	R^2	0.547

3.4 Effect of temperature on MB adsorption

Figure 5 illustrates MB removal and its adsorption capacity onto Fe-PAC at various temperature conditions. The trend of MB adsorption was improved with an increase in equilibrium temperature conditions. The average MB adsorption capacity was 101±3 mg/g under these experimental conditions. Concurrently, the removal efficiency of MB was 99.6% at 15 °C and slightly improved to 99.9% in the range of equilibrium temperature conditions between 25 °C and 65 °C. This can be explained by elevated equilibrium temperature conditions that may result in a swelling effect of Fe-PAC porosity, promoting a quick movement of MB molecules into internal pores of the adsorbent (Fu et al., 2015; Wu et al., 2014).

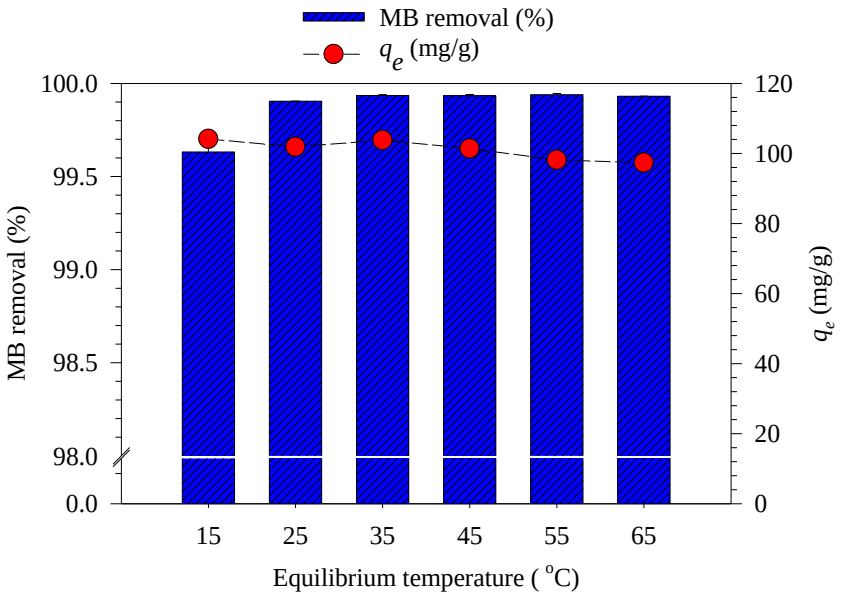

Figure 5. Influence of equilibrium temperature conditions on the adsorbed and removal efficiency of MB by Fe-PAC (Fe-PAC dosage of 2 g/L, initial MB concentration of 100 mg/L at initial pH of 6.16 and adsorption time of 20 h).

3.5 Adsorption thermodynamics

To further investigate the effect of temperature on the MB adsorption of Fe-PAC, thermodynamic analysis was carried out with its parameters presented in Table 3. Results revealed that there were negative values of ΔG^0 with these tested conditions indicating that the adsorption process of MB on Fe-PAC was spontaneous and thermodynamically feasible in nature. With the increase in equilibrium temperature conditions, more negative values of ΔG^0 were further increased from 288 K to 338 K, suggesting more efficient adsorption of MB at a higher temperature (Lalhmunsiama et al., 2016). This was consistent with the positive values of enthalpy change, (ΔH^0) which was found to be 23.28 kJ/mol, indicating the adsorption process was endothermic in nature and that higher temperature conditions also improve MB adsorption onto Fe-PAC. Comparatively, the calculated value of ΔS^0 was positive, confirming high affinity of Fe-PAC for MB molecules and increasing randomness at the solid-liquid interface during the sorption process (Nekouei et al., 2015).

Table 3. Thermodynamic parameters of MB adsorption onto Fe-PAC

Temperature (K)	ΔG^0 (kJ/mol)	ΔH^0 (kJ/mol)	ΔS^0 (kJ/mol)
288	-11.75	23.28	0.13
298	-15.51	-	-
308	-17.03	-	-
318	-17.51	-	-
328	-18.29	-	-
338	-18.50	-	-

4. CONCLUSIONS

In the present work, the iron oxide particles were successfully impregnated onto PAC. The prepared adsorbent Fe-PAC was used for MB adsorption in aqueous solution. Based on experimental results obtained from this study, MB molecules could be rapidly and efficiently removed by Fe-PAC adsorbent within a short contact time of 10 min at a MB adsorption capacity of 51 mg/g. The adsorption process of MB with Fe-PAC was well fitted by the pseudo-second-order-model, suggesting that chemisorption between MB molecules and adsorbent was estimated to be a rate-limiting step. Thermodynamic parameters indicated that MB adsorption onto Fe-PAC was feasible, endothermic and spontaneous in nature. Therefore, application of Fe-PAC adsorbent for MB adsorption was attractive, yielding benefits for treating dye-containing wastewater because of the favorable performance of Fe-PAC with MB removal and its easy separation from aqueous solution. Furthermore, the role of iron oxide particles on PAC should be investigated in future studies to differentiate MB removal rates and their adsorption capacity.

ACKNOWLEDGEMENTS

This study was developed within the scope of a project study of community water, sanitation and hygiene associated with diarrhea infection: A case study of Tha Song Yang District, Tak Province, Thailand, supported by a research grant from the Faculty of Tropical Medicine, Mahidol University, Fiscal year 2017-2019. The authors wish to thank the Coax Group Corporation Co., LTD, Thailand for their support and analysis of SEM micrographs. Many thanks to all staffs at Department of Social and Environmental Medicine, Faculty of Tropical Medicine, Mahidol University for supporting in this study. We would also like to express our deep thanks to Robert Sines and staffs from the Office of Research Services (ORS), Faculty of Tropical Medicine for their help with English editing of the manuscript.

REFERENCES

Abuzerr S, Darwish M, Mahvi AH. Simultaneous removal of cationic methylene blue and anionic reactive red 198 dyes using magnetic activated carbon nanoparticles: equilibrium, and kinetics analysis. Water Science and Technology 2018;2017(2):534-45.

Anjaneya O, Shrishailnath SS, Guruprasad K, Nayak AS, Mashetty SB, Karegoudar TB. Decolourization of Amaranth dye by bacterial biofilm in batch and continuous packed bed bioreactor. International Biodeterioration and Biodegradation 2013;79:64-72.

Borah D, Satokawa S, Kato S, Kojima T. Sorption of As (V) from aqueous solution using acid modified carbon black. Journal of Hazardous Materials 2009;162: 1269-77.

Fu J, Chen Z, Wang M, Liu S, Zhang J, Zhang J, Han R, Xu Q. Adsorption of methylene blue by a high-efficiency adsorbent (polydopamine microspheres): Kinetics, isotherm, thermodynamics and mechanism analysis. Chemical Engineering Journal 2015;259: 53-61.

Han Z, Sani B, Mrozik W, Obst M, Beckingham B, Karapanagioti HK, Werner D. Magnetite impregnation effects on the sorbent properties of activated carbons and biochars. Water Research 2015;70:394-403.

Ho Y, McKay G, Wase D, Forster C. Study of the sorption of divalent metal ions on to peat. Adsorption Science and Technology 2000;18:639-50.

Karcher S, Kornmüller A, Jekel M. Anion exchange resins for removal of reactive dyes from textile wastewaters. Water Research 2002;36:4717-24.

Kim S, Kim J, Seo G. Iron oxide nanoparticle-impregnated powder-activated carbon (IPAC) for NOM removal in MF membrane water treatment system. Desalination and Water Treatment 2013;51:6392-400.

Kitkaew D, Phetrak A, Ampawong S, Mingkhwan R, Phihusut D, Okanurak K, Polprasert C. Fast and efficient removal of hexavalent chromium from water by iron oxide particles. Environment and Natural Resources Journal 2018;16:91-100.

Lagergren S. About the theory of so-called adsorption of soluble substances. Sven. Vetenskapsakad. Handingarl 1898;24:1-39.

Lalhmunsiama, Tiwari D, Lee S-M. Surface-functionalized activated sericite for the simultaneous removal of cadmium and phenol from aqueous solutions: Mechanistic insights. Chemical Engineering Journal 2016;283:1414-23.

Li H, Dai M, Dai S, Dong X, Li F. Methylene blue adsorption properties of mechanochemistry modified coal fly ash. Human and Ecological Risk Assessment: An International Journal 2018;24:2133-41.

Lohwacharin J, Phetrak A, Oguma K, Takizawa S. Flocculation performance of magnetic particles with high-turbidity surface water. Water Science and Technology: Water Supply 2014;14:609-17.

Mohan D, Sarswat A, Singh VK, Alexandre-Franco M, Pittman Jr CU. Development of magnetic activated carbon from almond shells for trinitrophenol removal

from water. Chemical Engineering Journal 2011; 172:1111-25.

Naeem S, Baheti V, Wiener J, Marek J. Removal of methylene blue from aqueous media using activated carbon web. The Journal of The Textile Institute 2017;108:803-11.

Nekouei F, Nekouei S, Tyagi I, Gupta VK. Kinetic, thermodynamic and isotherm studies for acid blue 129 removal from liquids using copper oxide nanoparticle-modified activated carbon as a novel adsorbent. Journal of Molecular Liquids 2015;201:124-33.

Novais RM, Caetano APF, Seabra MP, Labrincha JA, Pullar RC. Extremely fast and efficient methylene blue adsorption using eco-friendly cork and paper waste-based activated carbon adsorbents. Journal of Cleaner Production 2018;197:1137-47.

Park HS, Koduru JR, Choo KH, Lee B. Activated carbons impregnated with iron oxide nanoparticles for enhanced removal of bisphenol a and natural organic matter. Journal of Hazardous Materials 2015;286:315-24.

Pathania D, Sharma S, Singh P. Removal of methylene blue by adsorption onto activated carbon developed from Ficus carica bast. Arabian Journal of Chemistry 2017;10:S1145-51.

Phihusut D, Chantharat M. Removal of methylene blue using agricultural waste: A case study of rice husk and rice husk ash from chaipattana rice mill demonstration center. Environment and Natural Resources Journal 2017;15:30-8.

Punyapalakul P, Takizawa S. Selective adsorption of nonionic surfactant on hexagonal mesoporous silicates (HMSs) in the presence of ionic dyes. Water Research 2006;40:3177-84.

Rajput S, Pittman CU, Mohan D. Magnetic magnetite (Fe_3O_4) nanoparticle synthesis and applications for lead (Pb^{2+}) and chromium (Cr^{6+}) removal from water. Journal of Colloid and Interface Science 2016; 468:334-46.

Rashidi HR, Sulaiman NMN, Hashim NA, Hassan CRC, Ramli MR. Synthetic reactive dye wastewater treatment by using nano-membrane filtration. Desalination and Water Treatment 2015;55:86-95.

Shang J, Pi J, Zong M, Wang Y, Li W, Liao Q. Chromium removal using magnetic biochar derived from herb-residue. Journal of the Taiwan Institute of Chemical Engineers 2016;68:289-94.

Suriyanon N, Permrungruang J, Kaosaiphun J, Wongrueng A, Ngamcharussrivichai C, Punyapalakul P. Selective adsorption mechanisms of antilipidemic and non-steroidal anti-inflammatory drug residues on functionalized silica-based porous materials in a mixed solute. Chemosphere 2015;136:222-31.

Weber WJ, Morris JC. Kinetics of adsorption on carbon from solution. Journal of the Sanitary Engineering Division 1963;89:31-60.

Wong KT, Eu NC, Ibrahim S, Kim H, Yoon Y, Jang M. Recyclable magnetite-loaded palm shell-waste based activated carbon for the effective removal of methylene blue from aqueous solution. Journal of Cleaner Production 2016;115:337-42.

Wu Z, Zhong H, Yuan X, Wang H, Wang L, Chen X, Zeng G, Wu Y. Adsorptive removal of methylene blue by rhamnolipid-functionalized graphene oxide from wastewater. Water Research 2014;67:330-44.